

**Novel Style of 2D Hofmann-Type Coordination Polymer
Incorporated Trigonal Prismatic Coordination Geometry
with Bidentate Co-Ligands**

Yuki Imamura^a, Haruka Yoshino^b, Benjamin Le Ouey^a, Ryo Ohtani^a
and Masaaki Ohba^{*a}

^a*Department of Chemistry, Faculty of Science, Kyushu University, 744 Motooka, Nishi-ku, Fukuoka 819-0395, Japan.*

^b*Institute for Materials Research, Tohoku University, 2-1-1 Katahira, Aoba-ku, Sendai 980-8577, Japan.*

Physical Measurement

Elemental analyses of carbon, hydrogen and nitrogen for **1** and **2** were carried out by the staff of technical support division graduate school of science, Kyushu University with J-SCIENCE LAB CHN simultaneous analyzer MICRO CORDER JM10 and JM11. Infrared (IR) spectra were performed on a Perkin Elmer Spectrum Two FT-IR equipped with an ATR accessory in the range of 650–4000 cm^{-1} at room temperature. Thermogravimetric analysis (TGA) was performed at a heating rate of $10^\circ\text{C min}^{-1}$ using a Rigaku Instrument Thermo plus TG 8120 at a nitrogen atmosphere. Energy dispersive X-ray fluorescence (XRF) analysis was conducted on a Shimadzu Rayny EDX-720 (X-ray voltage: 50 kV, X-ray current: 30 mA). Powder X-ray diffraction (PXRD) was carried out on a Rigaku Ultima IV diffractometer with graphite-monochromated $\text{Cu}_{K\alpha}$ radiation ($\lambda = 1.5418 \text{ \AA}$). Adsorption and desorption isotherms were collected using a BELSORP-MAX volumetric adsorption equipment (Microtrac BEL Corp.). The samples were activated by heating at 393 K for 24 h before the measurements. The magnetic properties were measured using a Quantum Design MPMS-XL5R SQUID. The samples were put into a gelatin capsule, placed in a plastic straw, and then fixed to the end of the sample transport rod. Diamagnetic correction was calculated by using Pascal constant.¹ The molar magnetic susceptibility ($\chi_M = M/H$) were corrected for the diamagnetism of the constituent atoms and the sample tube. The temperature dependence of field cooled magnetization (FCM) curve was gained in the temperature range of 2–50 K under an applied magnetic field of 10 Oe. The field dependence of magnetization curve was measured in the field range of -5 T to 5 T at 2 K. Temperature dependence of alternating-current (ac) magnetic susceptibilities ($\chi'_M =$ in phase, $\chi''_M =$ out of phase) were measured in the frequency range of 1–100 Hz under a zero dc field and an oscillating field of 3 Oe.

Single crystal X-ray diffraction

Single-crystal X-ray diffraction analysis of **1** was conducted on a Bruker SMART APEX II ULTRA CCD-detector Diffractometer, a rotating-anode (Bruker Turbo X-ray source) with graphite-monochromated MoK α radiation ($\lambda = 0.71073 \text{ \AA}$) was used. Computations were carried out on APEX2 crystallographic software package and OLEX2 software.² A single crystal was mounted on a polymer film with liquid paraffin and the temperature kept constant under flowing N₂ gas. The structure of **1** was solved by a standard direct method (XSHELL V6.3.1 crystallographic software package of the Bruker AXS) and expanded Fourier techniques. Full-matrix least-squares refinements were carried out with anisotropic thermal parameters for all non-disordered and nonhydrogen atoms. All hydrogen atoms were placed in the measured positions and refined using a riding model. Relevant crystal data collection and refinement data for the crystal structure data of **1** are summarized in Table S1 (CCDC 2304502).

Crystallography based on Rietveld refinement

A ground sample of **2** was sealed in a borosilicate glass capillary with an inner diameter of 0.2 mm. The synchrotron PXRD data ($\lambda = 1.138 \text{ \AA}$) for the structural analysis of **2** at 100 K was collected at BL-15 of the SAGA Light Source (SAGA-LS).³ The sample temperature was controlled by a dry N₂ flow using a Rigaku GN₂ apparatus. The PXRD pattern of **2** was indexed using FOX software,⁴ providing reasonable space group (*Pnma*) and cell parameters ($a = 14.3053(7) \text{ \AA}$, $b = 7.2469(2) \text{ \AA}$, $c = 17.0304(9) \text{ \AA}$ at 100 K) with the same orthorhombic system as that of **1** (Table. S2). The Rietveld refinement of **2** was carried out using RIETAN-FP and VESTA software,^{5,6} in which **1** was employed to construct the initial structural model. Refined parameters were as follows; 1) three peak-shift parameters, 2) twelve background parameters, 3) scale factor, 4) peak profile parameters with Split-Pearson VII function (three peak width parameters, three asymmetry parameters, and four decay parameters), 5) lattice constants (a , b , c), 6) overall isotropic atomic displacement parameter, and 7) fractional coordinates (x , y , z) for non-hydrogen atoms. All the parameters were refined under the soft constraints on bond distances and bond angles throughout the refinement. The hydrogen atoms were removed from the structural model in the initial stage of the refinement process. After the refinement of all parameters, hydrogen atoms were attached to the calculated positions, and then all parameters were refined. At the final refinement, all parameters except for lattice constants and scale factor were fixed to evaluate the standard error of the lattice constants. The refinement cycles were estimated from agreement factors of $R_{wp} = [\sum w[y - f(x)]^2 / \sum wy^2]^{1/2}$, where y and $f(x)$ represent the observed intensity and the calculated intensity at a diffraction angle of 2θ , respectively. $R_b = \sum ||F_o| - |F_c|| / \sum |F_o|$. Relevant crystal data collection and refinement data are summarized in Table S2 (CCDC 2304698).

Preparations

All chemicals were purchased from commercial sources and used without further purification. Precursor complexes, $(\text{PPh}_4)_2[\text{M}^{\text{V}}\text{N}(\text{CN})_4]\cdot 2\text{H}_2\text{O}$ ($\text{M} = \text{Cr}, \text{Mn}$) were prepared in accordance with literature procedure.⁷ Single crystals of **1** and powder samples of **2** were prepared by following procedures, respectively.

Single crystals of compound 1

The single crystals were prepared by a slow diffusion in a screw tube. An aqueous solution (1ml) of $\text{Mn}(\text{SO}_4)\cdot 5\text{H}_2\text{O}$ (1mg, 0.004mmol) was put at the bottom of tube. Then, a methanol solution (1ml) of dmbpy (0.7mg, 0.004mmol) and $(\text{PPh}_4)_2[\text{MnN}(\text{CN})_4]\cdot 2\text{H}_2\text{O}$ (3mg, 0.004mmol) was slowly layered on. After standing for several weeks, the pinkish-orange crystals were collected.

Elemental Analysis: Calcd for $\text{Mn}^{\text{II}}(\text{dmbpy})[\text{Mn}^{\text{V}}\text{N}(\text{CN})_4]$, $[\text{Mn}_2\text{C}_{16}\text{H}_{12}\text{N}_7]$: C, 46.62; H, 2.93; N, 23.79. Found: C, 46.38; H, 2.83; N, 23.61.

IR (cm^{-1}): 2156 ($\nu_{\text{C}\equiv\text{N}^-}$).

Powder samples of compound 2

All steps of this synthesis were carried out under N_2 gas flow. $(\text{PPh}_4)_2[\text{Cr}^{\text{V}}\text{N}(\text{CN})_4]\cdot 2\text{H}_2\text{O}$ (64mg, 0.075mmol), dmbpy (14mg, 0.075mmol), and $\text{Mn}(\text{NO}_3)_2\cdot 6\text{H}_2\text{O}$ (22mg, 0.075mmol) are dissolved in distilled acetonitrile (10ml), respectively. And then, the solution of dmbpy was added into the solution of $\text{Mn}(\text{NO}_3)_2\cdot 6\text{H}_2\text{O}$ while stirring. Subsequently, the solution of $(\text{PPh}_4)_2[\text{Cr}^{\text{V}}\text{N}(\text{CN})_4]\cdot 2\text{H}_2\text{O}$ was slowly dropped into the mixed solution with being stirred. After stirring over a day, pale-yellow powder was obtained and washed with acetonitrile. Yield: 27 mg (88%).

XRF analysis for **2**; $[\text{Mn}]/[\text{Cr}] = 1.12$.

Elemental Analysis: Calcd for $\text{Mn}^{\text{II}}(\text{dmbpy})[\text{Cr}^{\text{V}}\text{N}(\text{CN})_4]$, $[\text{MnCrC}_{16}\text{H}_{12}\text{N}_7]$: C, 46.96; H, 2.96; N, 23.96. Found: C, 45.18; H, 2.96; N, 22.63.

IR (cm^{-1}): 2168 ($\nu_{\text{C}\equiv\text{N}^-}$).

Table S1. Crystal parameters of **1**

	1
	CCDC 2304502
Formula	$C_{16}H_{12}N_7Mn_2$
Formula weight	412.190
Temperature / K	100
Crystal system	Orthorhombic
Space group	<i>Pnma</i>
<i>a</i> / Å	13.990
<i>b</i> / Å	7.058
<i>c</i> / Å	16.715
α / °	90
β / °	90
γ / °	90
<i>V</i> / Å ³	1650.46
<i>Z</i>	4
<i>R</i> ₁ / %	3.29
<i>wR</i> ₂ / %	8.64
Goodness of fit	1.048

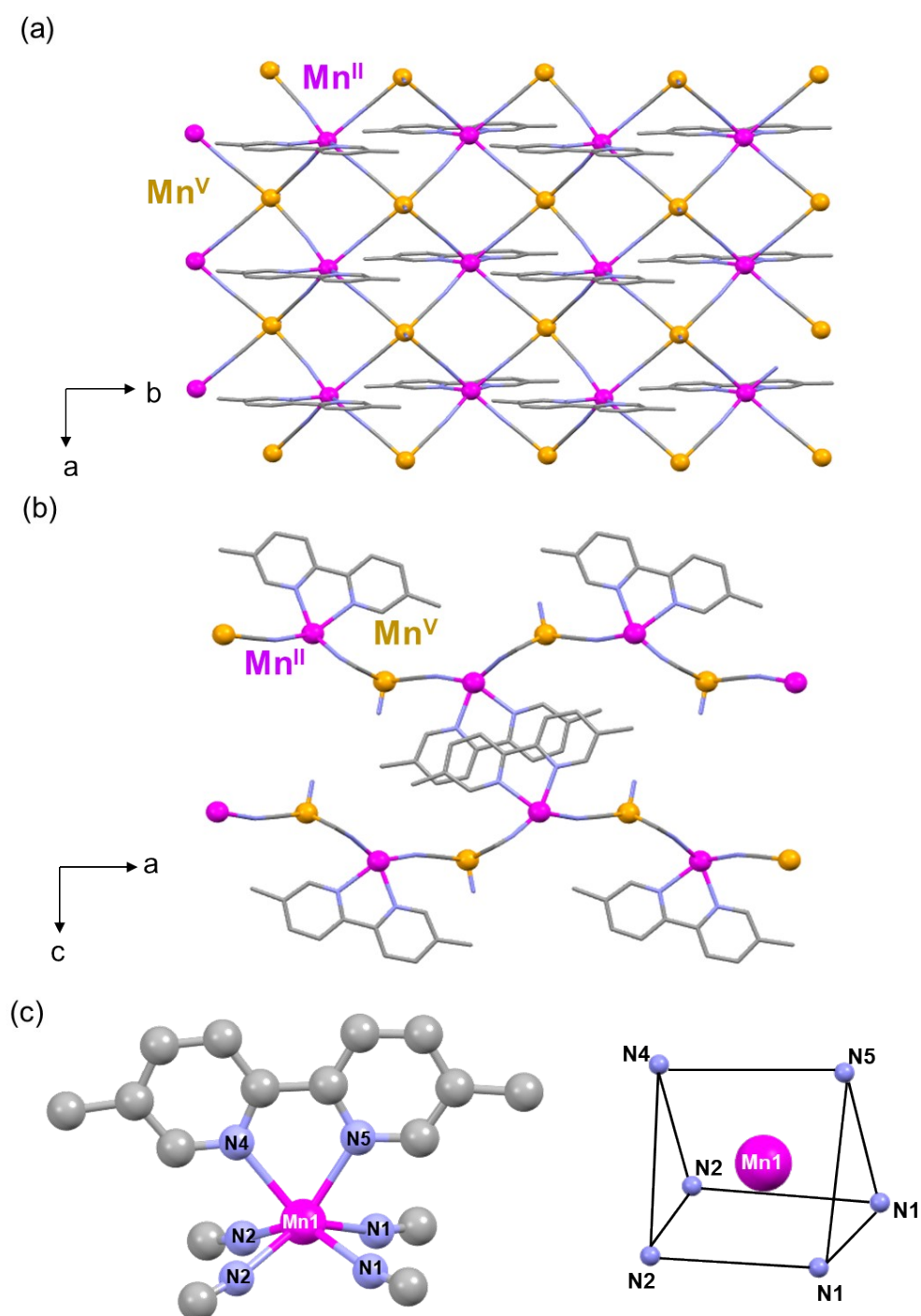


Figure S1. The crystal structure of **1** viewed along the (a) *c*- and (b) *b*-axis. (c) trigonal prismatic geometry of Mn^{II} ions in **1**. Color code: Mn^{II}, purple; Mn^V, orange; C, gray; N, blue, respectively. Hydrogen atoms were omitted for clarity.

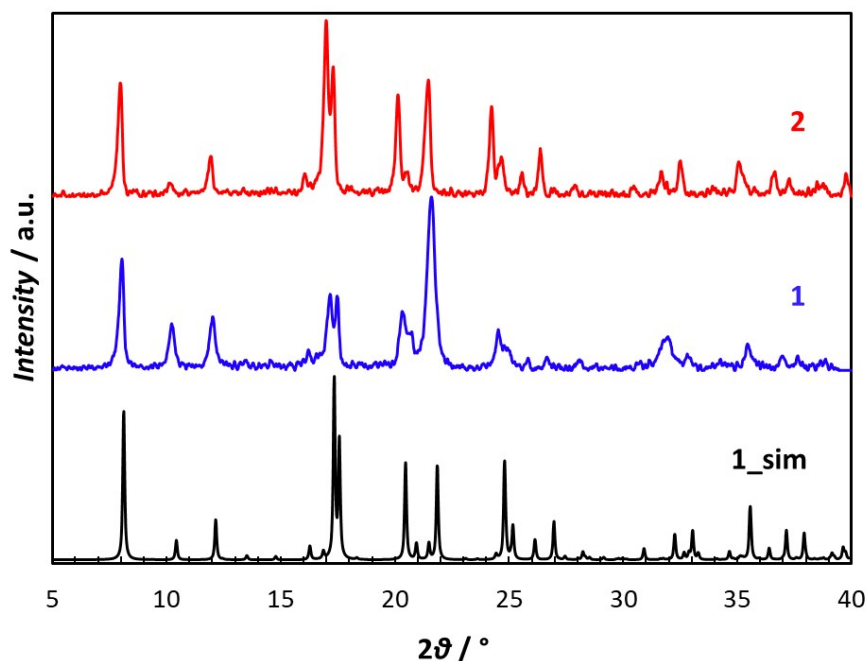


Figure S2. Powder X-ray diffraction (PXRD) patterns of as-synthesized samples of **1** (blue) and **2** (red), and the simulation pattern of **1** at 100K from SCXRD (black).

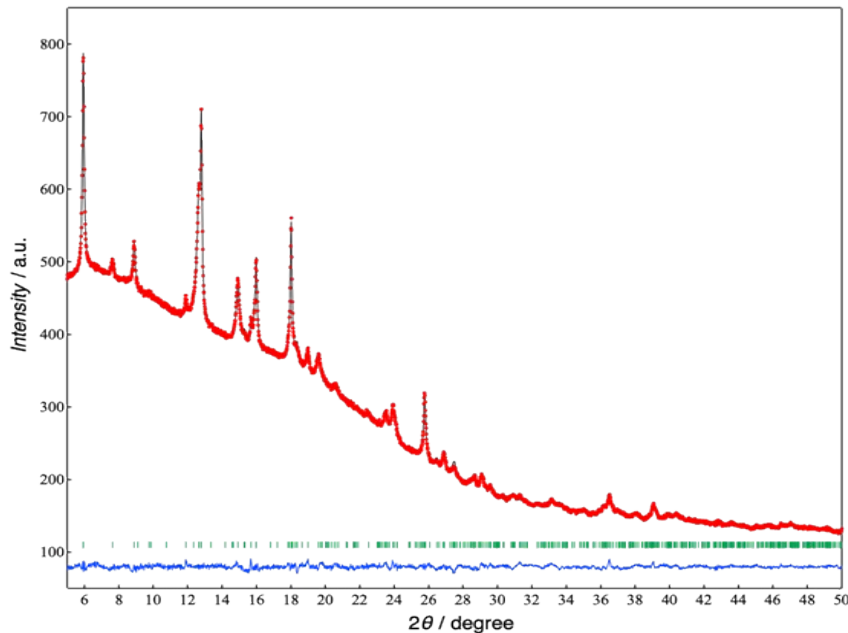


Figure S3. PXRD pattern ($\lambda = 1.138 \text{ \AA}$) and Rietveld refinement of **2**. Red dots, black line, and blue line represent the observed plots, calculated pattern, and their difference, respectively. Green bars are the calculated positions of the Bragg reflections.

Table S2. Crystal parameters of **2** obtained from Rietveld refinement.

	2
	CCDC 2304698
Formula	C ₁₆ H ₁₂ N ₇ MnCr
Formula weight	408.240
Temperature / K	100
Crystal system	Orthorhombic
Space group	<i>Pnma</i>
<i>a</i> / Å	14.3053(7)
<i>b</i> / Å	7.2469(2)
<i>c</i> / Å	17.0304(9)
α / °	90
β / °	90
γ / °	90
<i>V</i> / Å ³	1765.52(14)
<i>Z</i>	4
<i>D</i> _{calc} / g·cm ⁻³	1.536
<i>F</i> ₀₀₀	820
λ / Å	1.138
<i>R</i> _{wp} ^a	0.00868
<i>R</i> _B ^b	0.01064

^a $R_{wp} = [\sum w[y-f(x)]^2 / \sum wy^2]^{1/2}$, where *y* and *f*(*x*) represent the observed intensity and the calculated intensity at a diffraction angle of 2θ , respectively. ^b $R_B = \sum ||F_o| - |F_c|| / \sum |F_o|$.

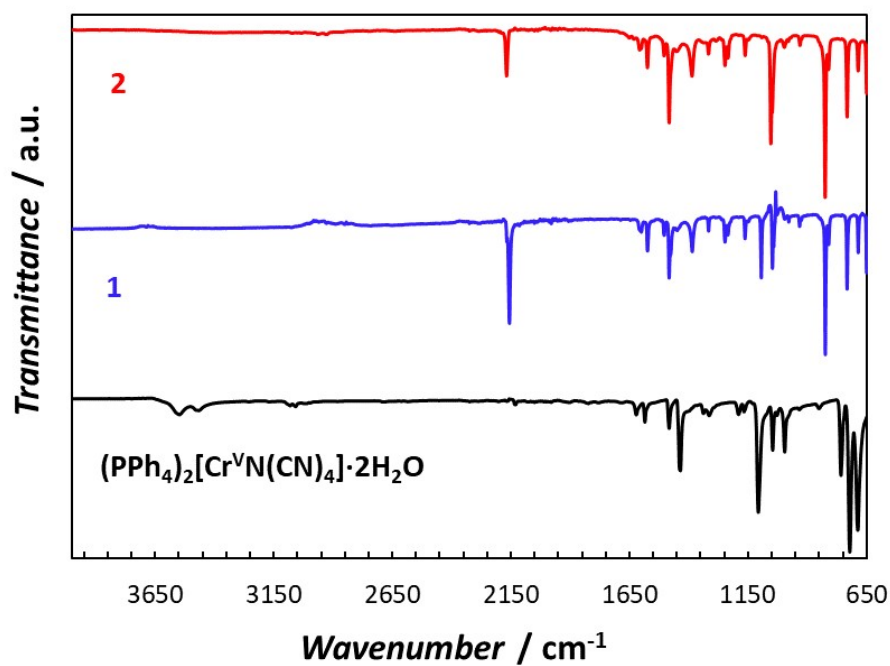


Figure S4. FT-IR spectra of **1** (blue), **2** (red) and the building unit, (PPh₄)₂[Cr^VN(CN)₄]·2H₂O (black).

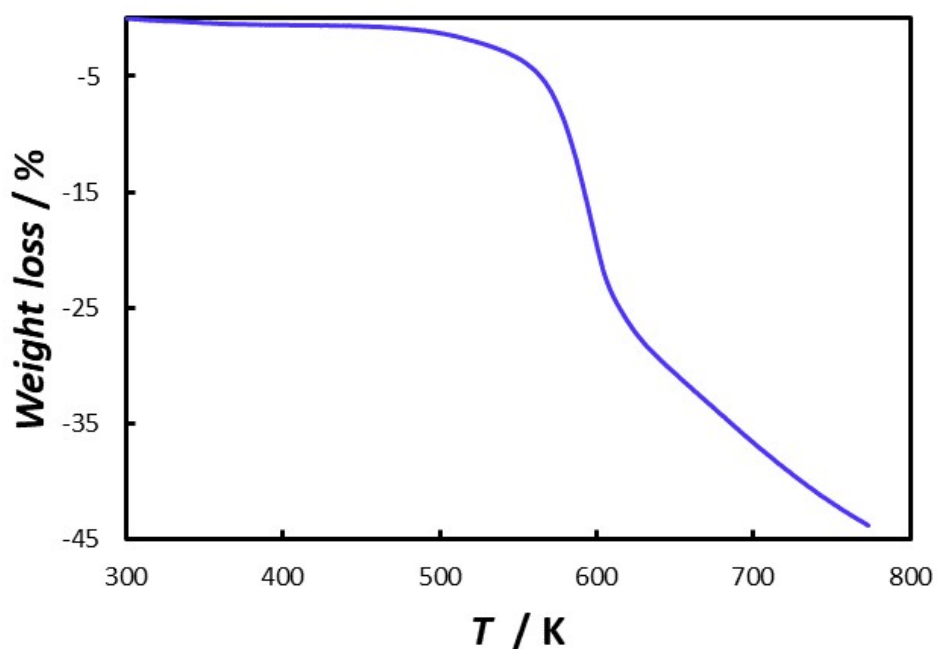


Figure S5. Thermogravimetric analysis curves of **2**. Heating rate was 10K/min under N₂ gas flow.

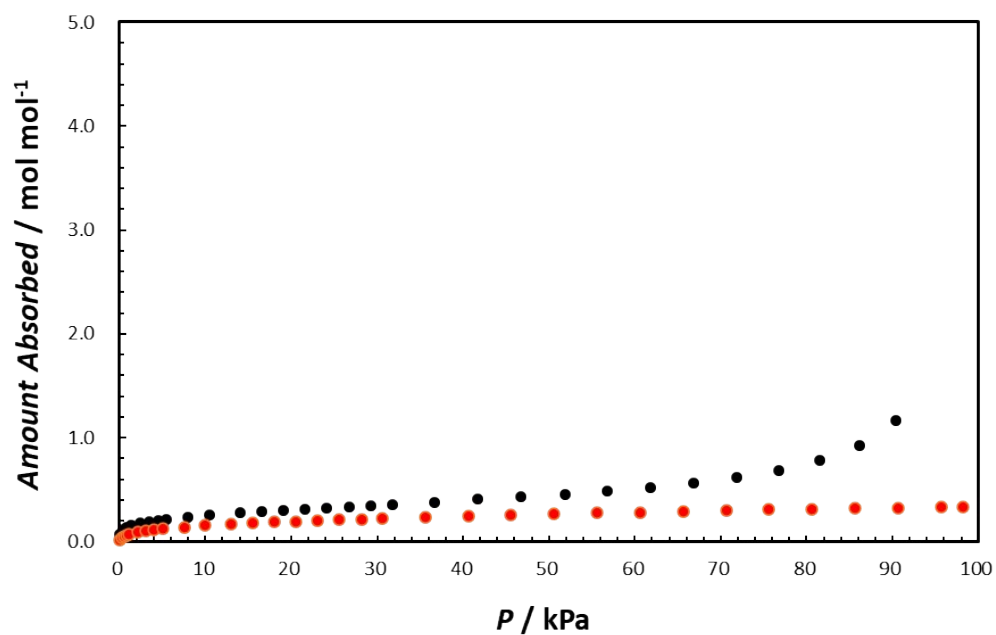


Figure S6. Adsorption (filled-circles) and desorption (open-circles) isotherms of **2** for N₂ (black) and CO₂ (red)

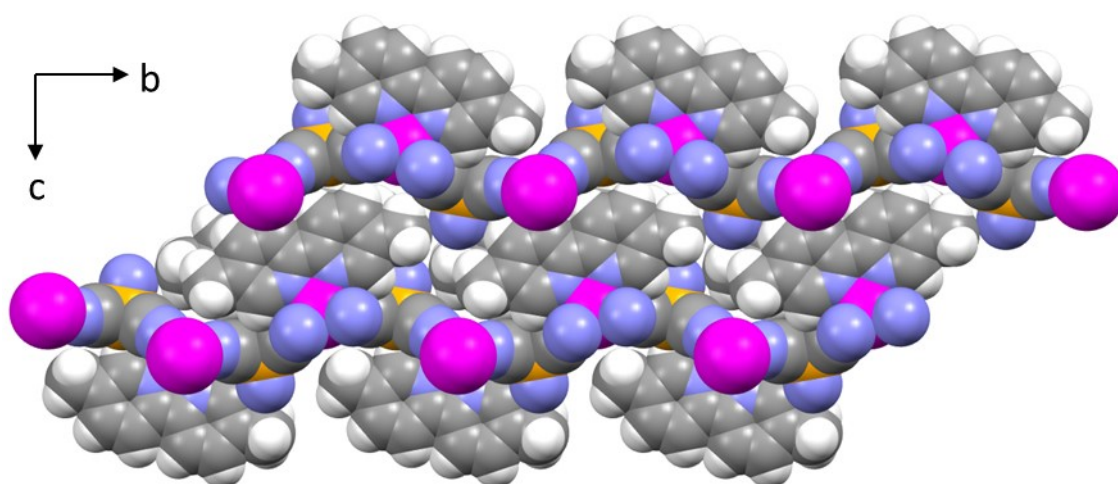


Figure S7. The space filling model of **1** obtained from SCXRD at 100K. Color code: Mn^V, orange; Mn^{II}, purple; C, gray; N, blue; H, white, respectively.

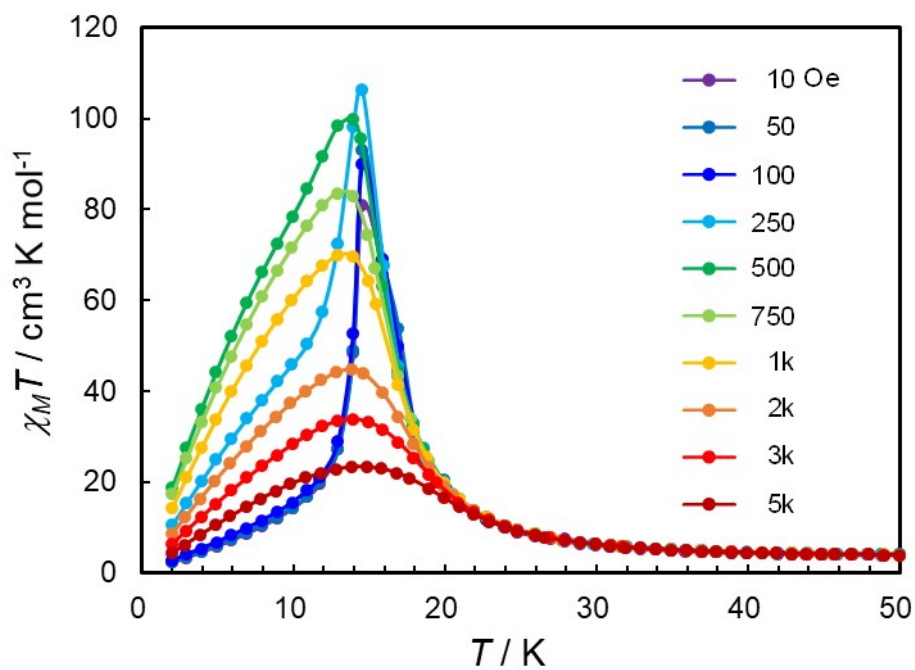


Figure S8. $\chi_M T$ vs. T plots at 50 - 2 K under the external magnetic field of 10–5k Oe.

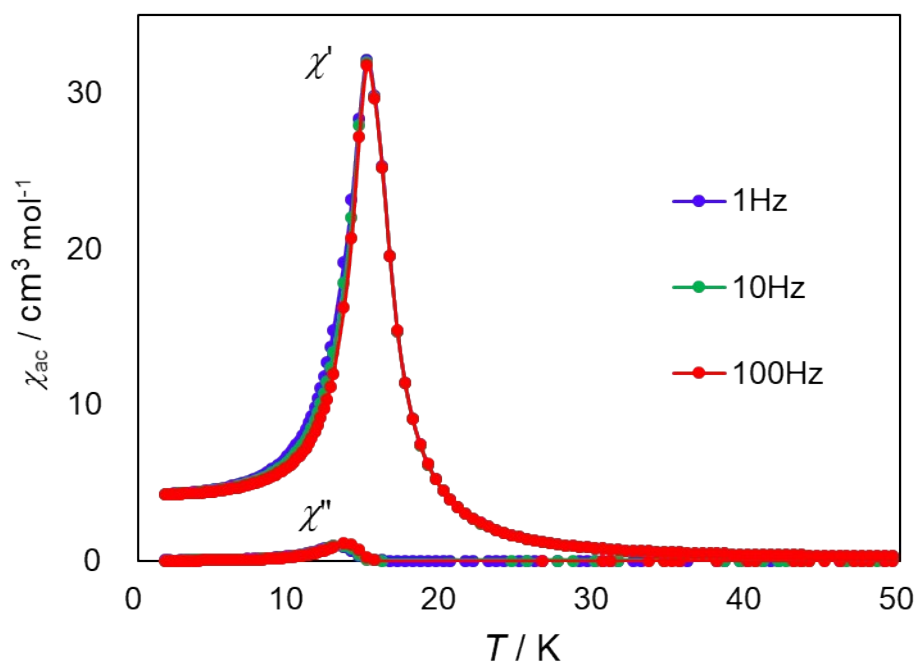


Figure S9. χ_M' vs. T and χ_M'' vs. T plots in frequency range of 1–100 Hz.

Reference

- 1 E. A. Boudreaux and L. N. Mulay, *Theory and Applications of Molecular Paramagnetism.*, (John Wiley & Sons, New York, 1976).
- 2 O. V. Dolomanov, L. J. Bourhis, R. J. Gildea, J. K. Howard and H. Puschmann, *J. Appl. Crystallogr.*, 2009, **42**, 339–341.
- 3 T. Okajima, Y. Chikaura, M. Tabata, H. Hashimoto, Y. Soejima, K. Hara and N. Hiramatsu, *Nucl. Instr. and Meth. in Phys. Res. B*, 2005, **238**, 185–188.
- 4 V. Favre-Nicolin and R. Černý, *J. Appl. Crystallogr.*, 2002, **35**, 734–743.
- 5 F. Izumi and K. Momma, *Solid State Phenom.*, 2007, **130**, 15–20.
- 6 K. Momma and F. Izumi, *J. Appl. Crystallogr.*, 2008, **41**, 653–658.
- 7 J. Bendix, K. Meyer, T. Weyhermuller, E. Bill, N. M. Nolte and K. Wieghardt, *Inorg. Chem.*, 1998, **37**, 1767-1775.